

Intermittency route to chaos for the nuclear billiard - a quantitative study

Daniel Felea*

Institute of Space Sciences, P.O.Box MG 23, RO 77125, Bucharest-Măgurele, Romania

Cristian Constantin Bordeianu, Ion Valeriu Grossu, Călin Beșliu, and Alexandru Jipa
Faculty of Physics, University of Bucharest, P.O.Box MG 11, RO 77125, Bucharest-Măgurele, Romania

Aurelian-Andrei Radu and Emil Stan

Institute of Space Sciences, P.O.Box MG 23, RO 77125, Bucharest-Măgurele, Romania

(Dated: June 19, 2018)

We extended a previous qualitative study of the intermittent behaviour of a chaotic nucleonic system, by adding a few quantitative analyses: of the configuration and kinetic energy spaces, power spectra, Shannon entropies, and Lyapunov exponents. The system is regarded as a classical "nuclear billiard" with an oscillating surface of a 2D Woods-Saxon potential well. For the monopole and dipole vibrational modes we bring new arguments in favour of the idea that the degree of chaoticity increases when shifting the oscillation frequency from the adiabatic to the resonance stage of the interaction. The order-chaos-order-chaos sequence is also thoroughly investigated and we find that, for the monopole deformation case, an intermittency pattern is again found. Moreover, coupling between one-nucleon and collective degrees of freedom is proved to be essential in obtaining chaotic states.

PACS numbers: 24.60.Lz, 05.45.-a, 05.45.Pq, 21.10.Re

I. INTRODUCTION

We begin by briefly reminding that a conjugated continuous effort has been made to relate the emergence of the collective energy dissipation through one and two-body nuclear processes with the chaotic behaviour of nuclear systems [1–34].

A few options in choosing the collective oscillation frequencies have come into focus in the past years, in connection with the onset of chaoticity for "nuclear billiards". First of all, the issue of dissipation into thermal motion of the adiabatic collective vibrational energy of the potential well was treated for several multipolarities by Burgio, Baldo *et al.* [1–3]. On the other hand, when trying to associate different vibration frequencies to various nuclear processes, the path to chaos was found to be changed with the order of multipole [29–34].

This paper was intended to bring a quantitative argumentation, based on a systematic study of the configuration and kinetic energy spaces, power spectra, informational entropies, and largest Lyapunov exponents. The study was done in completion of a few qualitative types of analysis previously presented [34]: sensitive dependence on the initial conditions, single-particle phase space maps, fractal dimensions of Poincare maps, and autocorrelation functions.

In short, we remind that, by studying the nucleonic dynamics in a Woods-Saxon potential, one can find an increase of the chaotic degree of the system behaviour as raising the frequency of 2D wall oscillation.

The main result of [34] was reported in relation with an intermittent route to chaos for the monopole vibrations close to the resonance phase of a nuclear interaction. Still, we mention that the purpose of these two coupled etudes was only to emphasize the detection of such intermission for the "nuclear billiards" and not to establish its type according to [35], nor to compare it with other intermittency patterns from known experimental results [36–45].

II. TOY MODEL

We continue the study on a classical dynamical system proposed by Burgio, Baldo *et al.* [1–3], system composed of a number of A nucleons with no charge, spin, or internal structure. A two-dimensional deep Woods-Saxon potential well, regarded as "nuclear billiard", is periodically hit by the nucleons. The Bohr Hamiltonian in polar coordinates is a sum of two components: kinetic ($E_{kin.}$) and potential ($E_{pot.}$), the kinetic one decoupling into radial (E_r), centrifugal (E_L), and collective terms ($E_{coll.}$):

$$E_{kin.} = E_r + E_L + E_{coll.} = \sum_{j=1}^A \left(\frac{p_{r_j}^2}{2m} + \frac{p_{\theta_j}^2}{2mr_j^2} \right) + \frac{p_\alpha^2}{2M}, \quad (1)$$

$$E_{pot.} = \sum_{j=1}^A V(r_j, R(\theta_j)) + \frac{M\Omega^2\alpha^2}{2}. \quad (2)$$

The phase space is defined by particle and collective momenta and their conjugate coordinates: (r, p_r) , (θ, p_θ)

*dfelea@spacescience.ro

and (α, p_α) . The collective coordinate α oscillates with Ω frequency, the Inglis mass M is equal to mAR_0^2 , and the nucleon mass: $m = 938$ MeV.

For the time being we are not interested in studying the nucleon dynamics beyond the Woods-Saxon barrier:

$$V(r_j, R(\theta_j)) = \frac{V_0}{1 + \exp\left[\frac{r_j - R(\theta_j, \alpha)}{a}\right]}, \quad (3)$$

and therefore we choose a deep well: $V_0 = -1500$ MeV and accordingly, a low value for the diffusivity coefficient: $a = 0.01$ fm.

When considering the two-dimensional case, the frontier of the collective motion is described as a function of the collective variable α and of the Legendre polynomials $P_L(\cos\theta_j)$ [1–3, 34]:

$$R_j = R(\theta_j, \alpha) = R_0 [1 + \alpha P_L(\cos\theta_j)]. \quad (4)$$

The oscillation degree of the potential well L is considered for the monopole (0), dipole (1) and quadrupole case (2).

If the surface has a stationary behaviour, or whenever one takes into account the uncoupled Hamilton equations (UCE) for the particle:

$$\dot{r}_j = \frac{p_{r_j}}{m}, \quad \dot{\theta}_j = \frac{p_{\theta_j}}{mr_j^2}, \quad \dot{p}_{r_j} = \frac{p_{\theta_j}^2}{mr_j^3} - \frac{\partial V}{\partial r_j}, \quad \dot{p}_{\theta_j} = -\frac{\partial V}{\partial R_j} \cdot \frac{\partial R_j}{\partial \theta_j}, \quad (5)$$

and collective degrees of freedom (*d.o.f.*):

$$\dot{\alpha} = \frac{p_\alpha}{M}, \quad \dot{p}_\alpha = -M\Omega^2\alpha - \sum_{j=1}^A \left(\frac{\partial V}{\partial R_j} \cdot \frac{\partial R_j}{\partial \alpha} \right), \quad (6)$$

R_0 has a fix value, chosen for consistency with previous papers [1–3, 34] as 6 fm.

A Runge-Kutta type algorithm (order 2-3) with an optimized step size was used for solving the system of differential equations, while keeping the absolute errors for the phase space variables under 10^{-6} and conserving the total energy with relative error: $\Delta E/E \approx 10^{-8}$ (Fig. 1).

We imposed the equilibrium condition between the pressure exerted by the particles and the mechanical pressure of the wall [1–3, 34] and thus obtained for the initial equilibrium value of the collective variable, perturbed with a small value:

$$\alpha_0 = \frac{-1 + \sqrt{1 + 8T/mR_0^2\Omega^2}}{2} + 0.15, \quad (7)$$

where $T = 36$ MeV [1–3, 34] is the two-dimensional kinetic energy and also the temperature of the nuclear system, when considering the natural system of units ($\hbar = c = k_B = 1$).

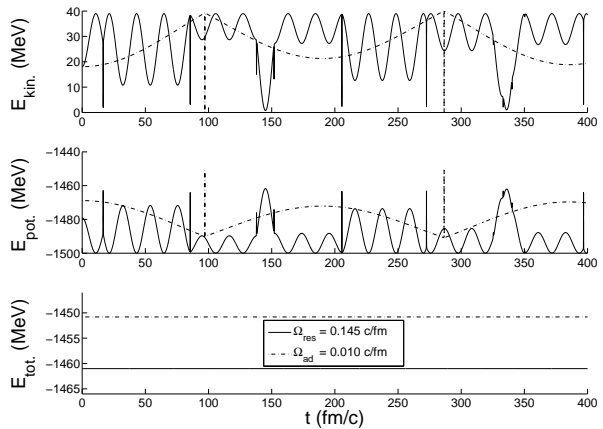


FIG. 1. Energy conservation for the adiabatic and resonance phase of the interaction ($L = 0$).

III. THE QUANTITATIVE ANALYSIS OF THE ROUTE TO CHAOS

We carry on the study begun in [34] by gradually changing the degree of vibration of the potential wall from a slow motion (adiabatic state) to a rapid one (the so-called resonance state of the interaction). In the first case, the collective motion is described by a radian frequency smaller than 0.05 c/fm. The latter is dominated by frequencies close to the one-nucleon collisional frequency:

$$\omega_{part} = \frac{\pi}{R_0} \cdot \sqrt{\frac{2T}{m}} \approx 0.145 \text{ c/fm}. \quad (8)$$

The physical motivation for studying the one-nucleon chaotic dynamics in the "nuclear billiard", ranging the frequencies from the adiabatic to the resonance regime of a nuclear interaction, is explained in some detail in [34].

We briefly remind that the process of nuclear multi-fragmentation can be viewed as a resonance process and that for smaller excitation energies, nuclear evaporation or breakup of a projectile nucleus occurs when the energy is shared between the collective and one-nucleon degrees of freedom.

By using a few types of analyses: sensitive dependence on the initial conditions, single-particle phase space maps, fractal dimensions of Poincare maps and autocorrelation functions, we emphasized that an intermittent route to chaos is observed in the monopole case when increasing the vibrational frequency to $\Omega = 0.1$ c/fm [34]. In the resonance phase of the interaction the onset of chaotic behaviour was found to be earlier than at any other adiabatic oscillations of the Woods-Saxon potential well.

We present here other methods [46] promoting the idea that the degree of chaoticity increases when moving from the adiabatic to the resonance regime: analyses of the

configuration and kinetic energy spaces, power spectra, generalized informational entropies and Lyapunov exponents. Furthermore, we try to identify possible pathways to chaos, including the intermittent one, previously put in evidence [34].

A. Configuration and kinetic energy spaces

In order to establish if a specific physical system presents a chaotic dynamics and to identify possible routes to chaos we analyzed the behaviour of a small bunch of trajectories in the configuration and in the kinetic energy space, respectively. For example, we took five trajectories separated by an $\epsilon = \Delta r = 0.01$ fm aperture, while keeping the rest of the initial phase space variables constant and let the system evolve over a given time ($\Delta t = 1,600$ fm/c).

For the transient stages from adiabatic to resonance, the temporal evolution of an initially confined trajectory bundle was studied for the monopole and dipole oscillation modes of the potential wall and also for the limit situation, in which the individual and collective degrees of freedom remain uncoupled (Figs. 2 and 3).

The configuration space revealed a high degree of symmetry in (r, θ) plane in both cases, $(4+2)$ uncoupled nonlinear differential equations and monopole (left and middle panels). Also, that the central zone remained uncovered, reflecting the conservation of the nucleon angular momentum.

Another important conclusion was issued from the definition of the stability concept of a dynamical system. For the aforementioned cases the dispersed trajectory pack periodically regroups on the frontier that delimits the forbidden zone of the phase space. This type of behaviour corresponds with the definition of stability given by Poisson (for e.g., in [47]). We will herewith remind that the Poisson stability defines as steady the movement of a particle system of which configuration comes close, from time to time, to the initial position.

At a first glance, on the simple UCE case one can distinguish two extremities of the radius of the particle periodic motion in the 2D potential well: $r_{min}(UCE) \approx 1.42$ fm, and $r_{Max}(UCE) \approx 5.96$ fm. These values correspond to the roots of the boundary equation:

$$E = \frac{p_\theta^2}{2mr^2} + V(r), \quad (9)$$

for a given one-nucleon energy E , when the radial component of velocity vanishes ($\dot{r}=0$).

The analysis of the particle motion in the configuration space is similar to that applied to any system with bound unclosed trajectories. The nucleonic motion takes place within a circular crown (the so-called *annulus*) determined by the concentric circles of r_{min} and r_{Max} radii. The trajectory is symmetric about any turning point.

For $\Delta t = 1,600$ fm/c we describe in the UCE case as much as 27 distinct apocenters (at $r = r_{Max}$). These are correlated with a number of 13 complete and one incomplete revolutions about the center of the force field (*i.e.* 27 straight lines before $r(t)$ changes its sense of variation).

The particle completely sweeps over twice the 2D configuration space after 1,537 fm/c. However, we notice that the bound trajectories are open, which means that the orbits never pass twice through a given point (see Fig. 2), which is in concordance with Bertrand's theorem. We briefly remind that for a bound orbit to be closed, the angle between two consecutive apocenters must be:

$$\Delta\theta = 2\pi \cdot \frac{n_1}{n_2}, \quad (10)$$

i.e. after n_2 revolutions about the center, the radius vector should sweep out a multiple n_1 of 2π radians. For the UCE case above considered we consequently obtain: $\Delta\theta_{UCE} \approx 4\pi/13$ radians (Fig. 2 - left column).

The kinetic energy points are displayed in right isocles triangular shaped patterns (Fig. 3), whose hypotenuses are described by Eqs. (11) and (12), for the two specific non-chaotical situations: UCE and the intermittent monopolar "window" emerged at $\Omega = 0.1$ c/fm:

$$E_{L_{UCE}} = 18.05 - E_r, \quad (11)$$

$$E_{L_{\Omega=0.1 \text{ c/fm}}} = 18.09 - E_r. \quad (12)$$

Moreover, for the intermittency frequency of monopole oscillations, one can notice a second smaller segment with the same negative slope:

$$E_{L_{\Omega=0.1 \text{ c/fm}}} = 5.87 - E_r. \quad (13)$$

For the uncoupled differential equations there are a couple of extreme values for the centrifugal kinetic energy: $E_{L_{min}}(UCE) = 1.02$ MeV, and $E_{L_{Max}}(UCE) = 18.05$ MeV, associated with $r_{Max}(UCE)$ and respectively, with $r_{min}(UCE)$ (left column of Fig. 3 and Eq. (1)).

As for the monopolar intermittency, we can distinguish just five distinct values for the E_L : 1.32 MeV, 2.13 MeV, 3.01 MeV, 5.87 MeV, and 18.09 MeV (central plot of Fig. 3), correlated with stationary radii: $r_1 \approx 5.26$ fm, $r_2 \approx 4.14$ fm, $r_3 \approx 3.49$ fm, $r_4 \approx 2.51$ fm, and $r_5 \approx 1.43$ fm (Eq. (1), Fig. 2 of [34], and central plot of Fig. 2). Thus, the nucleonic motion for the intermittent case is composed of alternated revolutions about the force field centre, forming a cyclic symmetrical structure, for e.g., $r_1, r_5, r_2, r_4, r_3, r_4, r_2, r_5, r_1$, and so on (Fig. 2). This behaviour can be easily verified through the sensitivity dependence on the initial conditions analysis, previously

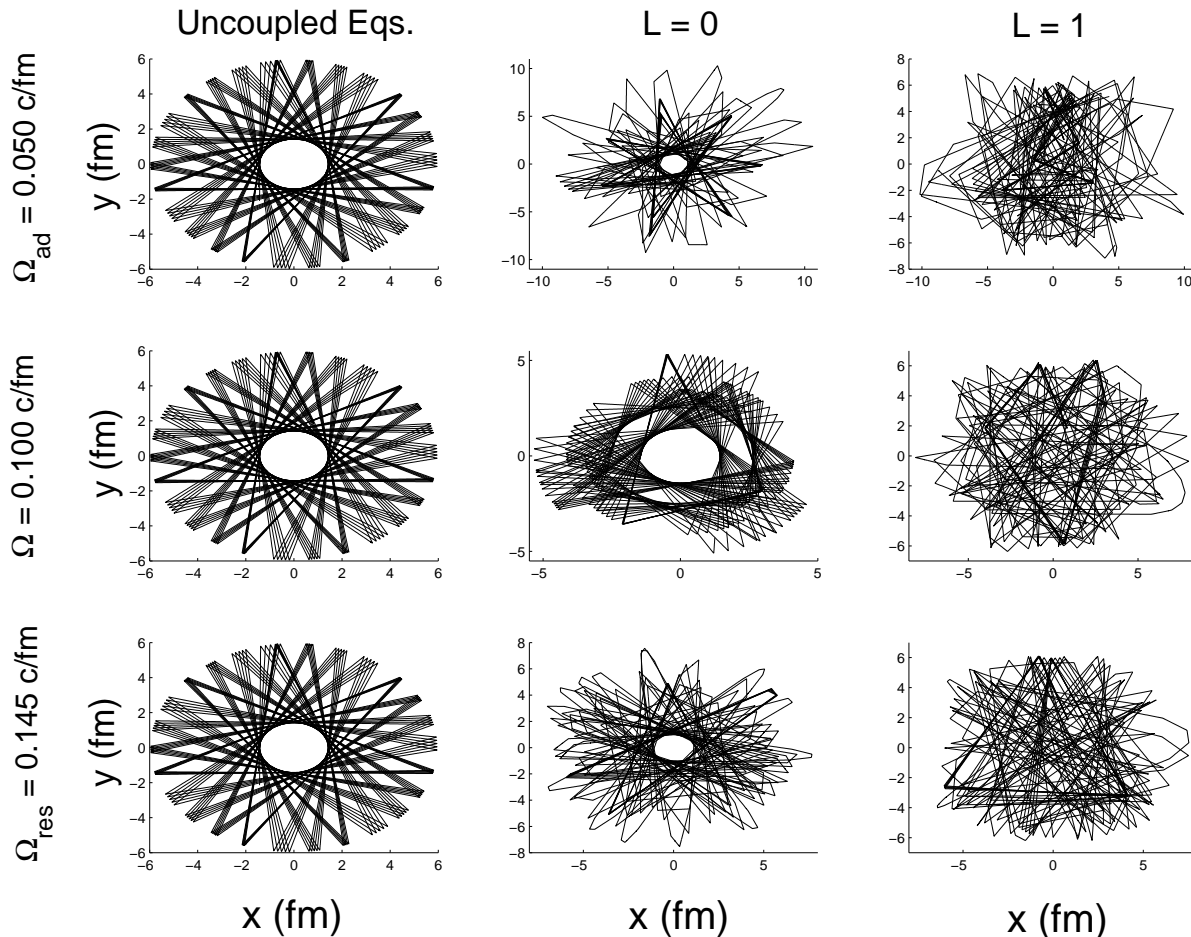


FIG. 2. The variance in time ($\Delta t = 1,600$ fm/c) of a packet of one-particle trajectories in the configuration space for adiabatic (upper row), intermediate (middle row), and resonance (lower row) collective vibrations for the uncoupled single and collective motion, monopole, and dipole cases.

presented (third column of Fig. 2 - [34]). It should also be mentioned that, following this radius alternation, the nucleon covers in 2D configuration space $\approx 2\pi$ radians after 6 full revolutions in almost 590 fm/c.

Concluding, we highlight once more, that ordered, non-chaotical events, exhibit periodical symmetrical patterns in the configuration and kinetic energy spaces. This was shown to be a characteristic feature of the uncoupled non-linear Hamilton equations case and also, of the steady, intermittent behaviour arisen in the monopole case at 0.1 c/fm vibrational radian frequency.

A tendency to compactly fill the kinetic energy space when increasing the monopolar vibrations (from 0.05 c/fm to 0.145 c/fm) was observed, except for the intermittency situation above described. For the $L = 1$ oscillation mode of the potential well, it seems that at the same frequency ($\Omega = 0.1$ c/fm) a somewhat intermittent behaviour could also come out, but this was proved to be elusive, as verified when reverting to this issue with the help of informational entropies and Lyapunov exponents

and analyzing the system on longer time periods.

B. Power spectra

In order to better distinguish between a multiple periodical behaviour that can also exhibit an erratic pattern and chaos we used the Fourier transform of the analyzed signals:

$$x(\omega) = \lim_{T \rightarrow \infty} \int_0^T e^{i\omega t} \cdot x(t) dt, \quad (14)$$

$$x(\omega) = \lim_{N \rightarrow \infty} \sum_{n=0}^N e^{i\omega t_n} \cdot x(t_n). \quad (15)$$

For a multiple periodical movement the power spectrum:

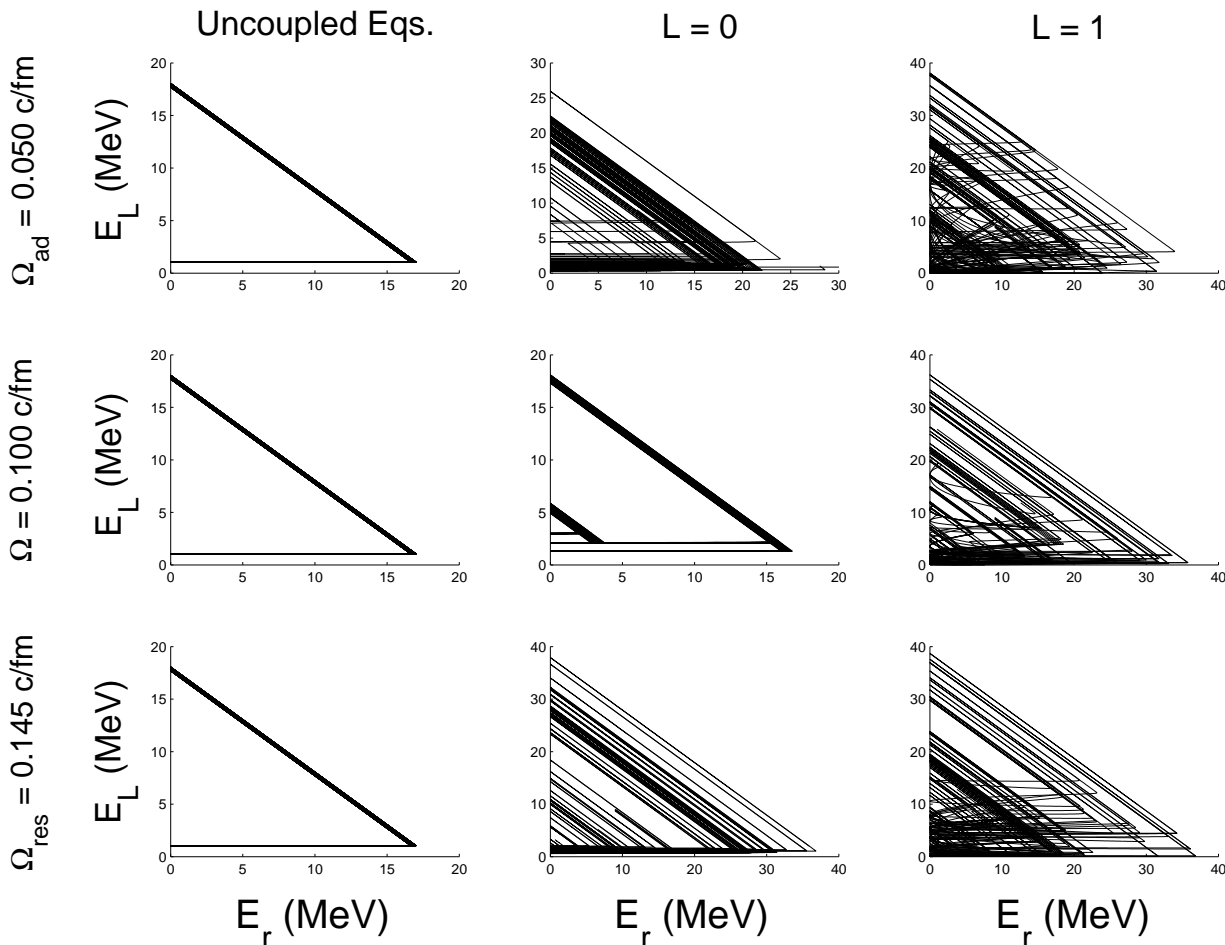


FIG. 3. The variance in time ($\Delta t = 1,600$ fm/c) of a packet of one-particle trajectories in the kinetic energy space for adiabatic (upper), intermediate (middle), and resonance (lower) collective vibrations for the uncoupled single and collective motion, monopole, and dipole cases.

$$P(\omega) = |x(\omega)|^2, \quad (16)$$

will only contain a number of discrete lines: the fundamental frequencies of the system and their associated sets of harmonics, while the chaotic behaviour is completely aperiodical and is represented by a continuous or quasi-continuous broadband.

The obtained results are presented in Figures 4-7. As a persistent feature of the physical system analyzed one should mention that for the monopole and dipole deformation degrees of the potential well (Figures 5 and 6) the chaotic behaviour increases in time, thus confirming previous results.

The transition towards a chaotic regime was put again in evidence once passing from the adiabatic to the resonance stage of the interaction. The power spectra reveal, as expected, the intermittent feature of the transition in the monopolar case at $\Omega = 0.1$ c/fm.

This can be detected for periods of time large enough

($\Delta t \geq 1,600$ fm/c) to positively identify chaotic patterns, by transition from a quasi-continuous spectrum of the one-nucleon radial coordinate ($\Omega_{ad} = 0.02$ c/fm) to a discrete periodical one, containing fundamental frequencies of the system and its harmonics ($\Omega = 0.1$ c/fm) and again to a continuous spectrum at the resonance vibrational frequency ($\Omega_{res} = 0.145$ c/fm) (Fig. 5 - right panels). The order-chaos-order-chaos sequence can be also spotted out for the monopole oscillations in the power spectra of the collective degree of freedom (Fig. 7 - second column).

The temporal series of the radius variable show a symmetrical sawtooth waveform for the uncoupled situation at any chosen vibration frequency, and also for the monopole case at adiabatic collective oscillations. For the rest, in general an asymmetrical sawtooth form defines the series, but sometimes, more complicated patterns appear at higher multipole orders (Figures 1-4 - [34]).

The difference between two successive maxima in the

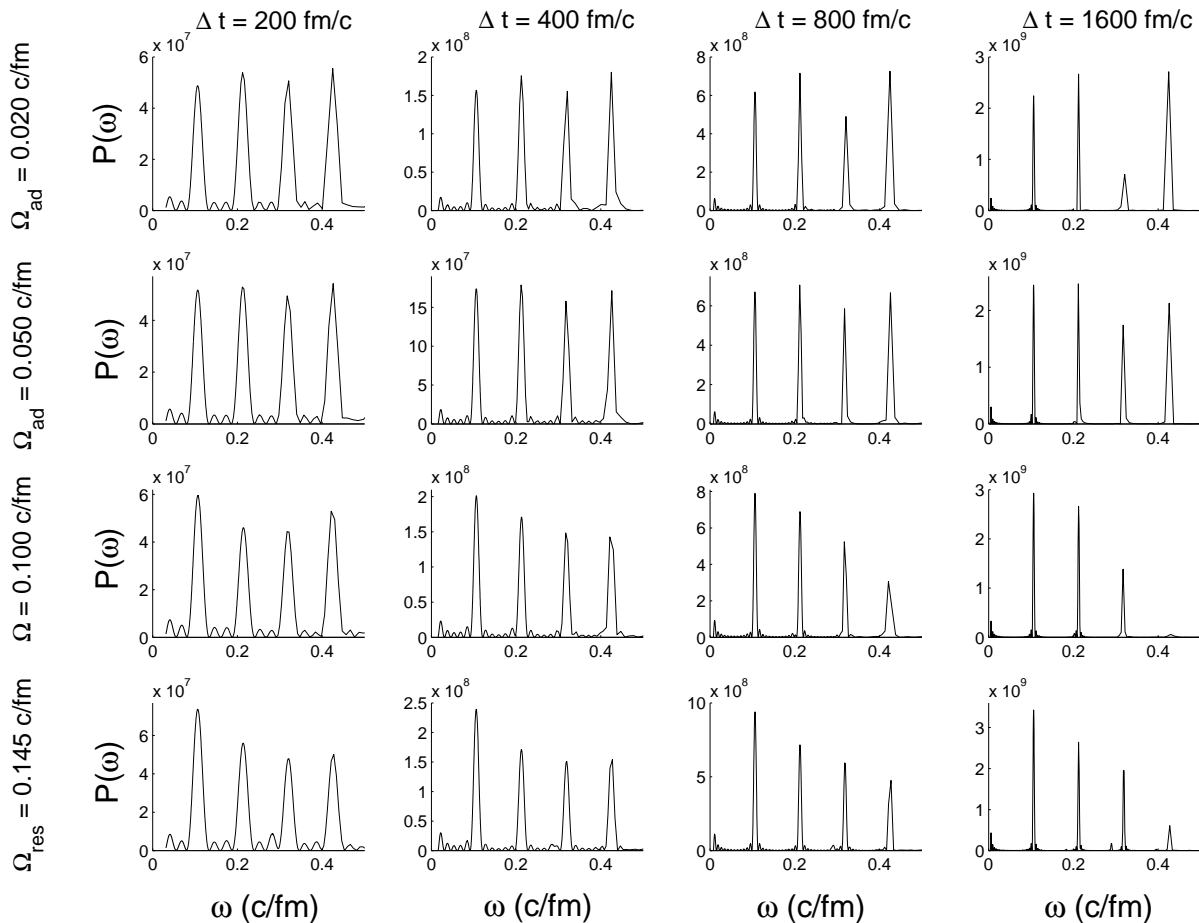


FIG. 4. The power spectra of the one-nucleon radial variable for different phases of the interaction (from adiabatic to resonance regime) calculated for the uncoupled single and collective degrees of freedom case.

temporal series of the radius variable for the UCE case is: $T_{0_{UCE}} \approx 1,537/26 = 59.1$ fm/c (left column of Fig. 2) and can be also obtained from the sensitive dependence on the initial conditions analysis (see Fig. 1 - [34]). The fundamental frequency for the radial sawtooth temporal series: $\omega_{0_{UCE}} = 2\pi/T_{0_{UCE}} = 0.106$ c/fm and its first three harmonics: $\omega_{1_{UCE}} = 0.212$ c/fm, $\omega_{2_{UCE}} = 0.318$ c/fm, and $\omega_{3_{UCE}} = 0.424$ c/fm, can be easily traced down in Figure 4.

As for the "window" of intermittency at $L = 0$, we obtained: $T_{0_{int}} \approx 590/12 = 49.2$ fm/c (Fig. 2 - [34] and central plot of current Fig. 2). This gives the corresponding fundamental frequency: $\omega_{0_{int}} = 0.128$ c/fm and its associated harmonics: $\omega_{1_{int}} = 0.256$ c/fm, $\omega_{2_{int}} = 0.384$ c/fm, and $\omega_{3_{int}} = 0.512$ c/fm (Fig. 5).

C. Shannon entropies

In order to further investigate route to chaos, we paid attention to the time evolution of the generalized infor-

mational entropy (or Shannon entropy), introduced as usually [46, 48–53]:

$$S_{Shannon}(t) = - \sum_{k=1}^{N(t)} p_k \cdot \ln p_k, \quad (17)$$

$N(t)$ being the number of gradually occupied cells until the time t .

This type of entropy is actually a number which quantifies the time rate of information production for a chaotic trajectory [17]. We consider in the first place the case of a particle that at every moment occupies a cell of the two-dimensional lattice phase space with a p_k probability:

$$p_k = 1/N_{total\ cells}, \quad (18)$$

where:

$$N_{total\ cells} = N_r \cdot N_{p_r} \cdot N_\theta, \quad (19)$$

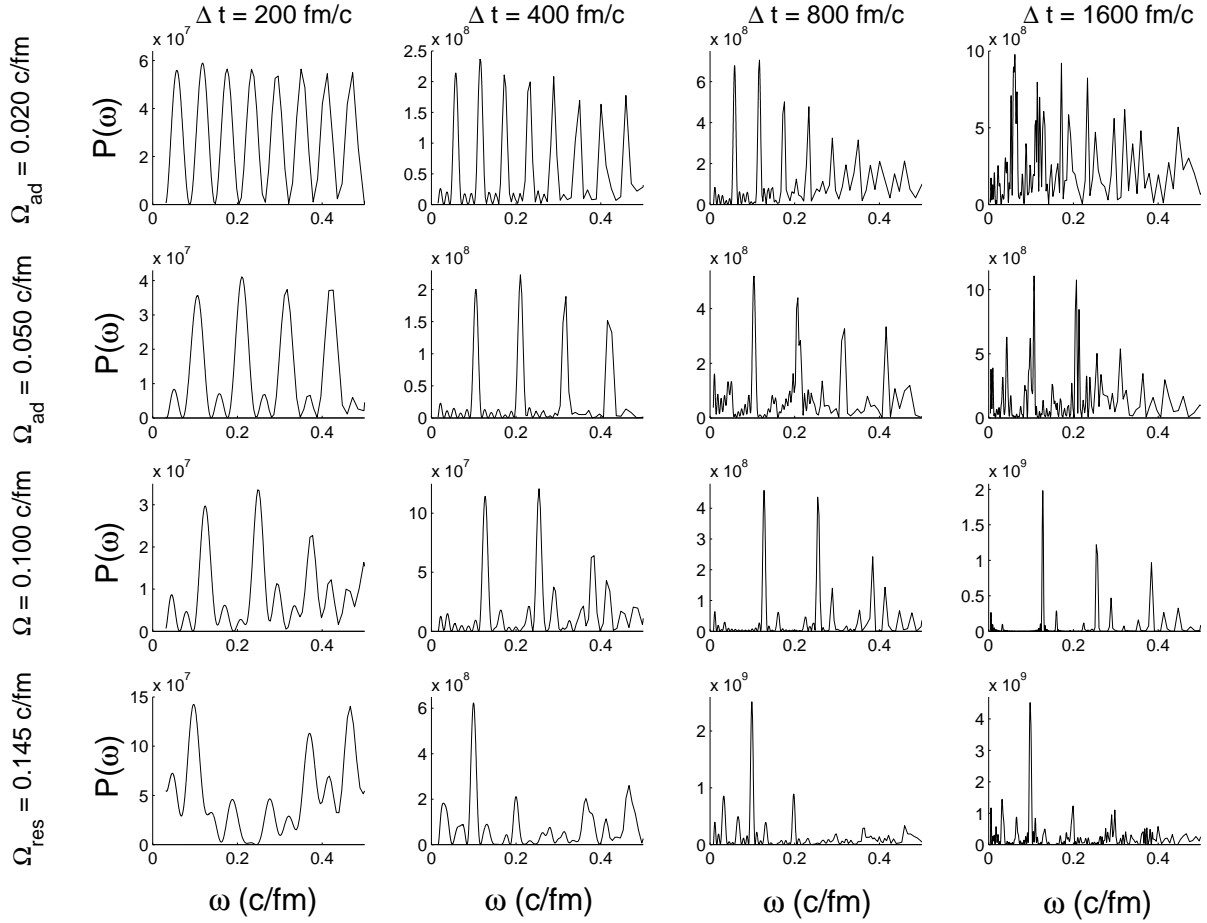


FIG. 5. The power spectra of the one-nucleon radial variable for different phases of the interaction (from adiabatic to resonance regime) calculated for the monopole case.

N_r , N_{p_r} , and N_θ are the number of bins of the (r, p_r, θ) lattice. For p_θ is a constant of motion for the monopole and the UCE cases, we use for comparisons only these three phase space variables.

As an alternative measure for the above defined entropy we also used the cumulative filling percentage of the one-nucleon phase space:

$$\eta(t) = \frac{N(t)}{N_{total\ cells}} \cdot 100 (\%). \quad (20)$$

In the first place, for a given wall frequency of vibration and for a certain multipolarity (here, for $\Omega_{res} = 0.145$ c/fm and $L = 0$), we studied the dependence of the Shannon entropy with the number of bins. A clear tendency for smoothing the entropy curve was found when decreasing the bin. A reduced number of cells ($N_b = 2^3$) is characterized by an entropy formed from a small number of high-amplitude Heaviside functions. As the number of bins increases (for e.g., here to 12^3), the entropy gets a more realistic representation, being composed of

a superior number of low-amplitude step functions (Fig. 8).

Moreover, the filling percentage η of the one-nucleon phase space maps can drastically differ with the size of the bin. Thus, after the system evolved over 400 fm/c, a phase space with 8 bins is entirely covered, 64 bins can be filled in with 0.8594 probability, a 26.95 filling percentage for 512 cells can be found, and we counted only as much as 226 bins occupied out of a total of 1,728 (*i.e.* $\eta = 13.08$ %).

At a first glance one can identify a series of entropy plateaus, which could be put in correspondence with stationary or quasi-stationary thermodynamic values of the system if a large number of particles would be under study. Some of them will vanish when considering a large number of bins. However, those surviving for $N_b \rightarrow \infty$ could be associated with stationary nucleonic states in the chosen potential well in the limit of a large number of degrees of freedom.

For a given 2D phase space lattice formed of $N_b = 4^3$ bins we present in Figures 9-12 a comparison between

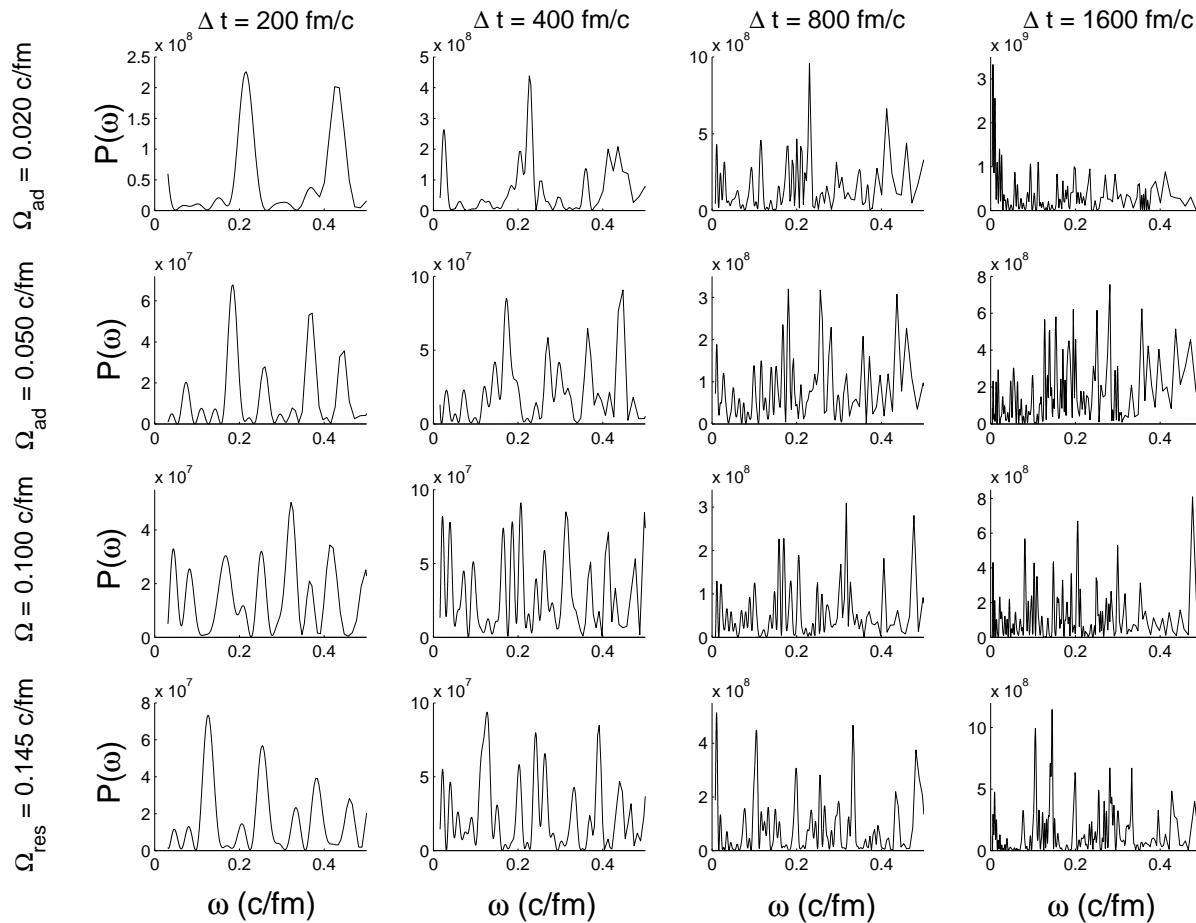


FIG. 6. The power spectra of the one-nucleon radial variable for different phases of the interaction (from adiabatic to resonance regime) calculated for the dipole case.

the informational entropies of the physical system in study, starting from the adiabatic stage of interaction and gradually increasing the vibrational wall frequency towards the dipole resonance value, $\Omega_{res} = 0.145$ c/fm. The slopes for the resonance frequency case were found to be significantly higher than for the adiabatic one ($\Omega_{ad} = 0.02$ c/fm) for all multipolarities involved.

Another comparison revealed significant differences between the onset times of the quasi-constant Shannon entropy values for all cases taken into consideration. Thus, for four vibrational radian frequencies and for four coupling modes of the Hamilton equations we show the informational entropy values after 800 fm/c (Table I) and the associated phase space filling degrees (Table II). Also, in Table III, are presented the periods of time after which the filling percentages η equal unity.

We continue the analysis by further defining the Shannon entropy for a group of w nearby orbits:

$$S_{traject. pack}(t) = \ln N_w(t), \quad (21)$$

TABLE I. The computed $S_{Shannon}(t = 800 \text{ fm/c})$ of the ($r \leftrightarrow p_r \leftrightarrow \theta$) one-particle phase space maps at several multipolarities and frequencies of wall vibration

Oscillation frequency	UCE	$L = 0$	$L = 1$	$L = 2$
$\Omega_{ad} = 0.020$ c/fm	3.6889	3.7136	3.7842	3.4340
$\Omega_{ad} = 0.050$ c/fm	3.6889	4.0775	4.0775	3.2958
$\Omega = 0.100$ c/fm	3.6889	3.6889	3.8501	4.0073
$\Omega_{res} = 0.145$ c/fm	3.6889	4.1589	4.0431	4.0254

so that the number of occupied cells is:

$$1 \leq N_w(t) \leq w, \quad (22)$$

thus describing the spread of the trajectories at each moment of time t (Figs. 13-16). When reaching the maximum divergence, the entropy for five distinct phase space paths gets its highest value (Table IV).

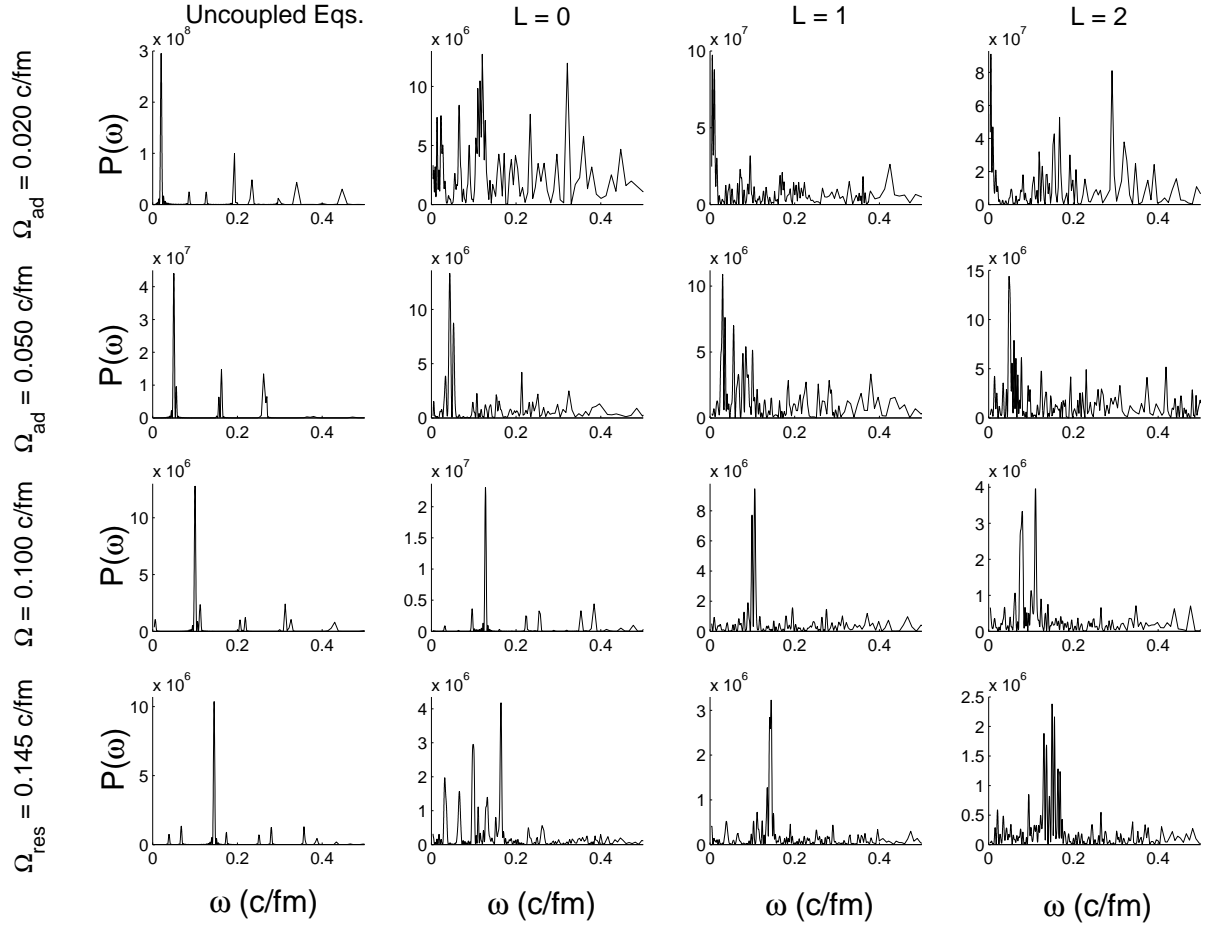


FIG. 7. The power spectra of the collective coordinate for different phases of the interaction (from adiabatic to resonance regime) calculated for the uncoupled single and collective degrees of freedom, monopole, dipole and quadrupole cases.

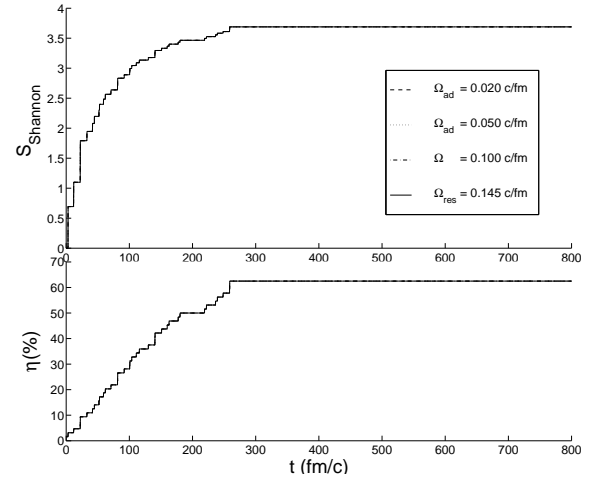
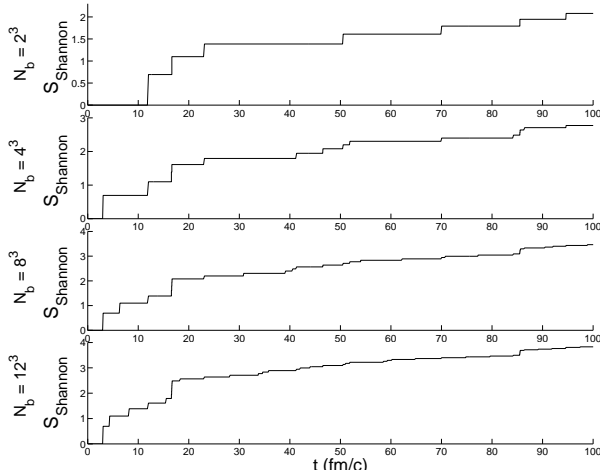


FIG. 8. The Shannon entropy (upper panel) and the filling degree of the one-particle phase space (lower panel) for all frequencies studied ($\Omega = 0.02 - 0.145$ c/fm), computed for the uncoupled single and collective degrees of freedom case.

FIG. 9. The Shannon entropy (upper panel) and the filling degree of the one-particle phase space (lower panel) for all frequencies studied ($\Omega = 0.02 - 0.145$ c/fm), computed for the uncoupled single and collective degrees of freedom case.

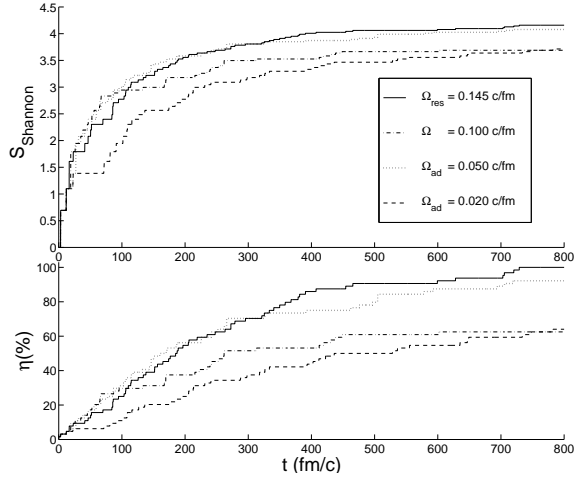


FIG. 10. The Shannon entropy (upper panel) and the filling degree of the one-particle phase space (lower panel) for all frequencies studied ($\Omega = 0.02 - 0.145$ c/fm), computed for the first degree of multipolarity ($L = 0$).

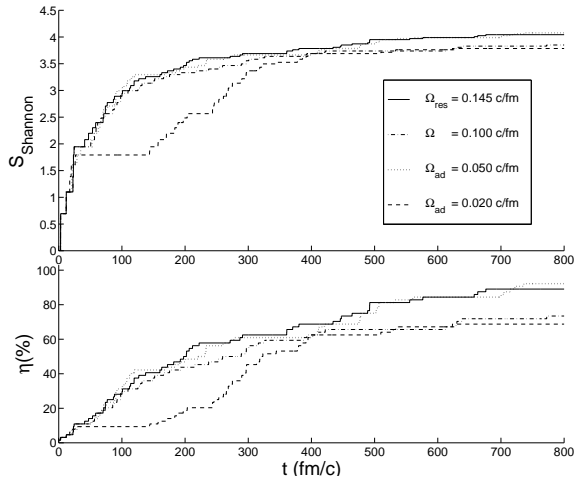


FIG. 11. The Shannon entropy (upper panel) and the filling degree of the one-particle phase space (lower panel) for all frequencies studied ($\Omega = 0.02 - 0.145$ c/fm), computed for the dipole case ($L = 1$).

TABLE II. The filling percentage η of the ($r \leftrightarrow p_r \leftrightarrow \theta$) one-particle phase space maps at several multiplicities and frequencies of wall vibration

Oscillation frequency	UCE	$L = 0$	$L = 1$	$L = 2$
$\Omega_{ad} = 0.020$ c/fm	62.50	64.06	68.75	48.44
$\Omega_{ad} = 0.050$ c/fm	62.50	92.19	92.19	42.19
$\Omega = 0.100$ c/fm	62.50	62.50	73.44	85.94
$\Omega_{res} = 0.145$ c/fm	62.50	100.00	89.06	87.50

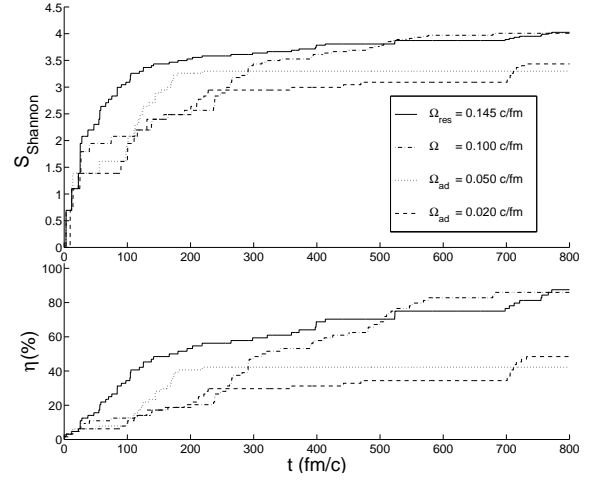


FIG. 12. The Shannon entropy (upper panel) and the filling degree of the one-particle phase space (lower panel) for all frequencies studied ($\Omega = 0.02 - 0.145$ c/fm), computed for the quadrupole oscillations ($L = 2$).

TABLE III. The time (in fm/c) at which the informational entropies of the ($r \leftrightarrow p_r \leftrightarrow \theta$) one-particle phase space maps at several multiplicities and frequencies of wall vibration have the maximum value (*i.e.* $\eta = 100$ %)

Oscillation frequency	UCE	$L = 0$	$L = 1$	$L = 2$
$\Omega_{ad} = 0.020$ c/fm	$> 10^5$	6, 023	6, 359	5, 356
$\Omega_{ad} = 0.050$ c/fm	$> 10^5$	1, 618	4, 223	$> 10^5$
$\Omega = 0.100$ c/fm	$> 10^5$	11, 442	3, 241	2, 758
$\Omega_{res} = 0.145$ c/fm	$> 10^5$	729	1, 887	10, 571

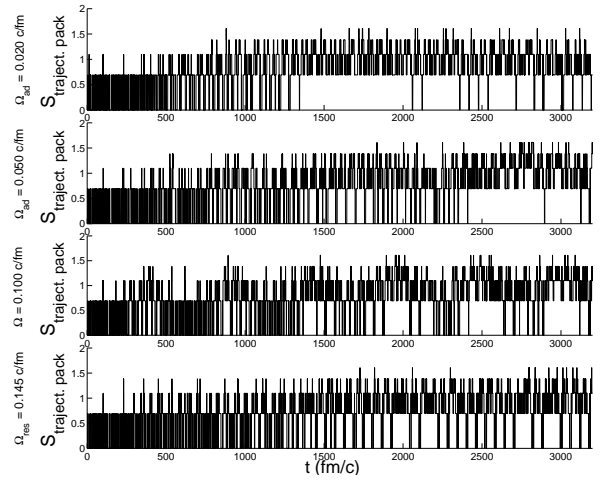


FIG. 13. The Shannon entropy of a bunch of five one-particle close trajectories for frequencies between 0.02 and 0.145 c/fm (uncoupled single and collective degrees of freedom case).

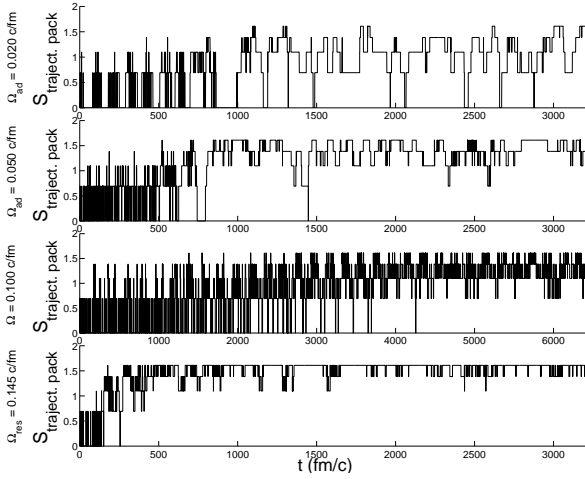


FIG. 14. The Shannon entropy of a bunch of five one-particle close trajectories for frequencies between 0.02 and 0.145 c/fm ($L = 0$).

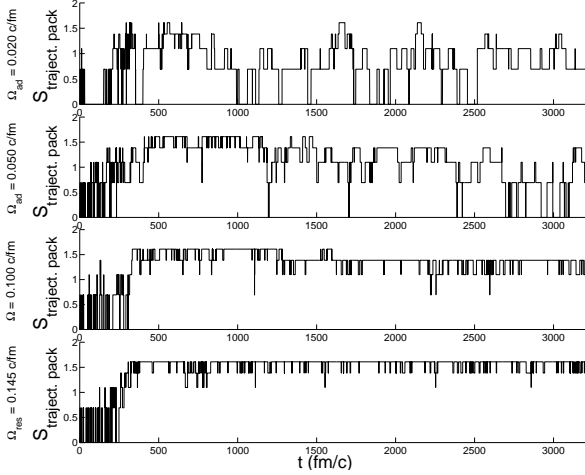


FIG. 15. The Shannon entropy of a bunch of five one-particle close trajectories for frequencies between 0.02 and 0.145 c/fm ($L = 1$).

TABLE IV. The time (in fm/c) at which the one-particle Shannon entropies of a pack of $w = 5$ close orbits begin having the maximum value (*i.e.* $S_{traject. pack} = 1.60944$) for various coupling degrees between the one-nucleon and the collective *d.o.f.* and for the standard chosen wall frequencies

Oscillation frequency	UCE	$L = 0$	$L = 1$	$L = 2$
$\Omega_{ad} = 0.020$ c/fm	$> 10^4$	1,095	555	688
$\Omega_{ad} = 0.050$ c/fm	$> 10^4$	855	476	122
$\Omega = 0.100$ c/fm	$> 10^4$	4,133	333	395
$\Omega_{res} = 0.145$ c/fm	$> 10^4$	279	327	469

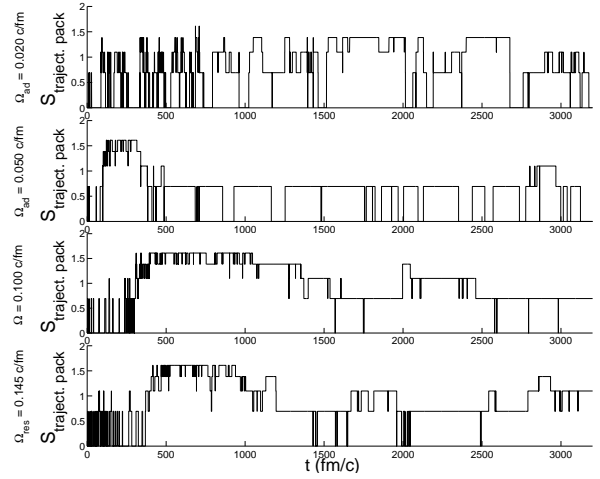


FIG. 16. The Shannon entropy of a bunch of five one-particle close trajectories for frequencies between 0.02 and 0.145 c/fm ($L = 2$).

We begin the analysis with the UCE case. The single and collective uncoupled *d.o.f.* give birth to a quasi-laminar behaviour with a weak development of chaotic states. The one-particle informational entropy shows an identical evolution, no matter the frequency chosen. The orbit covers, after 800 fm/c, only 62.50 % of the entire lattice (Table II and Figure 9) and does not reach 100 %, even after $\Delta t = 100,000$ fm/c (Table III). Also, the phase space is not covered up by all five trajectories for the whole range of 10,000 fm/c considered, when analyzing $S_{traject. pack}$ (Fig. 13 and Table IV).

For the dipole oscillations mode, at $\Omega_{ad} = 0.05$ c/fm, it appears that, after only 800 fm/c, the entropy closes in upon its maximum value: $S_{Max} = \ln N_{total cells} = 4.1589$ (Fig. 11 and Table I). However, on long periods of time, the real tendency is towards filling up the nucleonic phase space as rapid as the vibrational frequency is increased (Table III). The exact pattern is repeated when studying the Shannon entropy for closeby nucleonic trajectories (Fig. 15 and Table IV).

We found quite the same feature for the monopole case, with exception for the intermittent "window" at $\Omega = 0.1$ c/fm (Tables I, II and Fig. 10). The occupying rate is so small in the intermittent zone, that just at 11,442 fm/c, the particle would have covered the whole phase space (see Table III). A similar conclusion can be drawn from Table IV and Fig. 14 (with a double temporal scale scanned for the intermittent frequency). The trajectory pack informational entropy reaches its highest value after the longest one-particle evolution time of all: 4,133 fm/c.

The quadrupole oscillation also reveals an apparent intermittent pattern, this time at $\Omega_{ad} = 0.05$ c/fm. We call it intermittent because after 800 fm/c the nucleon fills in only 42.19 % of the total number of bins (Figure 12 and Table II), and a longer time than 100,000 fm/c is required to get to $\eta = 100$ % (Table III). However, this

behaviour can be a misleading one, the Shannon entropy for a trajectory bunch showing exactly the opposite (see Fig. 16 and Table IV), after 122 fm/c the orbits being completely dispersed.

D. Lyapunov exponents

We furthermore presented another quantitative analysis: the temporal evolution of the Lyapunov exponents, $\lambda(t)$. As previously shown, initial adjacent points in the phase space $\Delta x_0(t=0)$, can generate in time separated trajectories $\Delta x(t)$. When studying the evolution of a single phase space parameter, the one-dimensional Lyapunov exponent takes the form:

$$\lambda(t) = \lim_{|\Delta x_0| \rightarrow 0} \ln \left| \frac{\Delta x(t)}{\Delta x_0} \right|. \quad (23)$$

The generalization for obtaining the multi-dimensional Lyapunov exponent is then straightforward:

$$\lambda(t) = \ln \frac{\left(\sum_{k=1}^m [x_k(t) - x_{k0}]^2 \right)^{\frac{1}{2}}}{0.01}, \quad (24)$$

where the sum is taken over all $m = 4$ squared differences between final $x_k(t)$ and initial x_{k0} one-nucleon phase space variables. Integration times of the order of 10^3 fm/c exclude errors when computing the Lyapunov exponents.

In short, we here remind that the trajectories can be classified as function of the Lyapunov exponents. Thus, one can distinguish periodical behaviours, for $\lambda = 0$, dissipative movements with a fixed point or a basin of attraction ($\lambda < 0$), and aperiodical chaotic states ($\lambda > 0$), when the iterative discrete evolution of the solution series (Eqs. 5 and 6) leads to a chaotic pattern.

Another way of measuring the system sensitivity to initial conditions is to compute the largest Lyapunov exponent (LLE). Usually a couple of methods can be employed, one based on the time dependence of the multi-dimensional Lyapunov exponent, the other on Wolf's standard method that uses a Gram-Schmidt Reorthonormalization of the tangent vectors [54]. In the latter, the LLE is obtained by taking the asymptotic value of the multi-dimensional Lyapunov exponent:

$$\lambda_{Max} = \lim_{t \rightarrow \infty} \frac{\lambda(t)}{t}. \quad (25)$$

Still, this method has the disadvantage that the integration times have to be at least an order of magnitude larger than those here considered. Other methods are slightly less efficacious, being more CPU time-consuming when simulating strong chaotic systems [55].

We consequently used the first method and noticed the saturation behaviour, *i.e.* the arising of a plateau after

TABLE V. The largest Lyapunov exponents (in c/fm) computed as slopes of the increasing branches of the ordinary Lyapunov exponents for the degrees of multipole and vibrational frequencies used

Oscillation frequency	$L = 0$	$L = 1$	$L = 2$
$\Omega_{ad} = 0.020$ c/fm	0.003939	0.008689	0.004306
$\Omega_{ad} = 0.050$ c/fm	0.004432	0.009829	0.023203
$\Omega = 0.100$ c/fm	0.000761	0.015454	0.014402
$\Omega_{res} = 0.145$ c/fm	0.008739	0.016662	0.010086

a certain time t_c (Fig. 17). The straight lines represent fits whose slopes match the LLE (Table V). They are in inverse proportion with the onset times of chaoticity ($\tau = 1/\lambda_{Max}$), being a measure of the trajectory decoupling at a microscopic level.

When the single-particle and collective *d.o.f.* remain uncoupled, the Lyapunov exponents basically oscillate between two quasi-stationary regimes. This happens for all vibrational frequencies involved, reflecting a periodical regrouping of orbits in two basins of attraction. The phase space not being covered, even after a hundred of thousand of fm/c, computing the LLE becomes futile for this case.

One can remark for dipole oscillations (Fig. 17 - middle column) a faster evolution towards reaching saturation states of the 4-dimensional Lyapunov exponents, once passing from the adiabatic ($\tau_{ad} = 115$ fm/c) to the resonance phase of the interaction ($\tau_{res} = 60$ fm/c).

In the monopolar case the intermittency can be easily traced at 0.1 c/fm vibrational frequency (Fig. 17 - left panels). During the intermittent stage, independent nearby orbits microscopically diverge with the slowest rate of all: $\tau = 1,314$ fm/c (Table V). In order to catch the heaving in sight of the stationary plateau at $\approx 4,917$ fm/c, the temporal scale was scanned over 6,400 fm/c.

The study of the quadrupole collective oscillation case confirms the results obtained with all previous analyses. Namely, the neighbouring trajectories deviate one from each other after just 43 fm/c at an adiabatic frequency: 0.05 c/fm. Also, when increasing Ω , the LLE evolution pattern exactly matches that found with informational entropy measured for a group of orbits (Tables IV and V).

IV. CONCLUSIONS

We investigated the chaotic nucleonic behaviour in a two-dimensional deep Woods-Saxon potential well for specific phases of the nuclear interaction. By comparing the order-to-chaos transition for these cases of interest, from adiabatic to resonance regime, it was shown that the couplings between the one-particle dynamics and

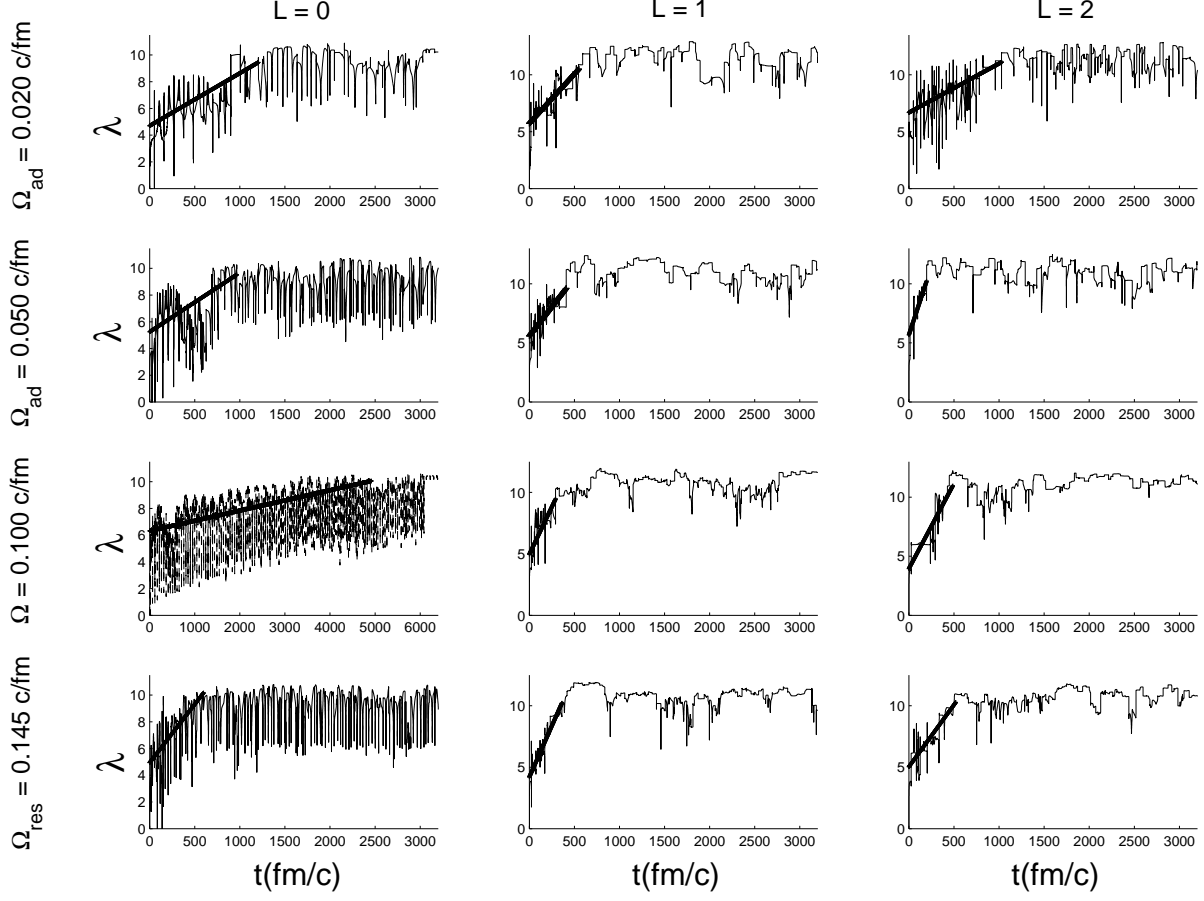


FIG. 17. The temporal evolution of the Lyapunov exponents of the single-particle *d.o.f.* for multiple radian frequencies Ω and multipolarities L of the nuclear surface. The LLE are given by fits (thickened solid lines) of the increasing portions of the 4-dimensional Lyapunov exponents.

high multipole vibrational modes significantly decrease the onset of the chaotic nucleonic motion towards realistic nuclear interaction time scale.

The quantitative study enfolded a plethora of analyses, pointing out that the paths to chaos for the "nuclear billiard" are dissimilar for the studied multipolarities. For the first two multipole degrees we noticed a more rapid emergence of chaotic states as moving on towards higher radian frequencies of oscillation. When analyzing the system with quadrupole collective deformations of the potential well, an order-strong chaos-weak chaos-order sequence is revealed. Still, as emphasized in the "Shannon entropies" subsection, the quadrupole case represents an intricate one, and further analysis would be required before concluding it.

Every type of quantitative analysis strengthened previous results regarding the monopolar intermittency route to chaos for the "nuclear billiard". The collective os-

cillation frequency for the intermittent behaviour was located prior to the resonance state of interaction (at $\Omega = 0.1$ c/fm).

Further studies along the above issues are currently in progress. The used formalism can be improved by adding spin and charge to the nucleons. A semi-quantal treatment of this problem, including Pauli blocking effect, is hoped to shed more light on the discussed issue in the near future.

ACKNOWLEDGMENTS

We wish to thank to R.I. Nanciu, I.S. Zgură, A.Ş. Cârstea, G. Păvălaş, S. Zaharia, A. Gheţă, M. Rujoiu, A. Mitruţ, and R. Mărginean for fruitful discussions on this paper.

- [1] G.F. Burgio, M. Baldo, A. Rapisarda, and P. Schuck, Phys. Rev. C **52**, 2475 (1995).
- [2] M. Baldo, G.F. Burgio, A. Rapisarda, and P. Schuck, in *Proceedings of the XXXIV International Winter Meeting on Nuclear Physics, Bormio, Italy, 1996*, edited by I. Iori. arXiv:nucl-th/9602030
- [3] M. Baldo, G.F. Burgio, A. Rapisarda, and P. Schuck, Phys. Rev. C **58**, 2821 (1998).
- [4] J. Blocki, Y. Boneh, J.R. Nix, J. Randrup, M. Robel, A.J. Sierk, and W.J. Swiatecki, Ann. Phys. (N.Y.) **113**, 330 (1978).
- [5] P. Ring and P. Schuck, *The Nuclear Many Body Problem* (Springer-Verlag, Berlin, 1980) p. 388.
- [6] J. Speth and A. van der Woude, Rep. Prog. Phys. **44**, 719 (1981).
- [7] C.Y. Wong, Phys. Rev. C **25**, 1460 (1982).
- [8] P. Grassberger and I. Procaccia, Phys. Rev. Lett. **50**, 346 (1983).
- [9] M. Sieber and F. Steiner, Physica D **44**, 248 (1990).
- [10] A. Rapisarda and M. Baldo, Phys. Rev. Lett. **66**, 2581 (1991).
- [11] A.Y. Abul-Magd and H.A. Weidenmüller, Phys. Lett. B **261**, 207 (1991).
- [12] J. Blocki, F. Brut, T. Srokowski, and W.J. Swiatecki, Nucl. Phys. A **545**, 511c (1992).
- [13] R. Blümel and J. Mehl, J. Stat. Phys. **68**, 311 (1992).
- [14] M. Baldo, E.G. Lanza, and A. Rapisarda, Chaos **3**, 691 (1993).
- [15] J. Blocki, J.J. Shi, and W.J. Swiatecki, Nucl. Phys. A **554**, 387 (1993).
- [16] M.V. Berry and J.M. Robbins, Proc. R. Soc., London, Sect. A **442**, 641 (1993).
- [17] E. Ott, *Chaos in Dynamical Systems* (Cambridge University Press, Cambridge, England, 1993).
- [18] W. Bauer, D. McGrew, V. Zelevinsky, and P. Schuck, Phys. Rev. Lett. **72**, 3771 (1994).
- [19] R. Hilborn, *Chaos and Nonlinear Dynamics* (Oxford University Press, Oxford, England, 1994).
- [20] R. Blümel and B. Esser, Phys. Rev. Lett. **72**, 3658 (1994).
- [21] S. Drozdz, S. Nishizaki, and J. Wambach, Phys. Rev. Lett. **72**, 2839 (1994).
- [22] S. Drozdz, S. Nishizaki, J. Wambach, and J. Speth, Phys. Rev. Lett. **74**, 1075 (1995).
- [23] W. Bauer, D. McGrew, V. Zelevinsky, and P. Schuck, Nucl. Phys. A **583**, 93 (1995).
- [24] C. Jarzynski, Phys. Rev. Lett. **74**, 2937 (1995).
- [25] A. Bulgac and D. Kusnezov, Chaos, Solitons and Fractals **5**, 1051 (1995).
- [26] A. Atalmi, M. Baldo, G.F. Burgio, and A. Rapisarda, Phys. Rev. C **53**, 2556 (1996). arXiv:nucl-th/9509020
- [27] A. Atalmi, M. Baldo, G.F. Burgio, and A. Rapisarda, in *Proceedings of the XXXIV International Winter Meeting on Nuclear Physics, Bormio, Italy, 1996*, edited by I. Iori. arXiv:nucl-th/9602039
- [28] P.K. Papachristou, E. Mavrommatis, V. Constantoudis, F.K. Diakonou, and J. Wambach, Phys. Rev. C **77**, 044305 (2008). arXiv:nucl-th/0803.3336
- [29] D. Felea, C. Beşliu, R.I. Nanciu, Al. Jipa, I.S. Zgură, R. Mărginean, M. Haiduc, A. Gheată, and M. Gheată, in *Proceedings of the 7th International Conference "Nucleus-Nucleus Collisions", Strasbourg, 2000*, edited by W. Norenberg *et al.* (North-Holland, Amsterdam, The Netherlands, 2001) p. 222.
- [30] D. Felea, *The Study of Nuclear Fragmentation Process in Nucleus-Nucleus Collisions at Energies higher than 1 A GeV*, Ph.D. thesis, University of Bucharest, Faculty of Physics (2002) p. 134.
- [31] C.C. Bordeianu, C. Beşliu, Al. Jipa, D. Felea, and I.V. Grossu, Comput. Phys. Commun. **178**, 788 (2008).
- [32] C.C. Bordeianu, D. Felea, C. Beşliu, Al. Jipa, and I.V. Grossu, Comput. Phys. Commun. **179**, 199 (2008).
- [33] C.C. Bordeianu, D. Felea, C. Beşliu, Al. Jipa, and I.V. Grossu, Rom. Rep. in Phys. **60**, 287 (2008).
- [34] D. Felea, I.V. Grossu, C.C. Bordeianu, C. Beşliu, Al. Jipa, A.A. Radu, C.M. Mitu, and E. Stan, "Intermittency route to chaos for the nuclear billiard - a qualitative study", Phys. Rev. C (submitted).
- [35] Y. Pomeau and P. Manneville, Commun. Math. Phys. **74**, 189 (1980).
- [36] P. Berge, M. Dubois, P. Manneville, and Y. Pomeau, J. Phys. (Paris) **41**, L344 (1980).
- [37] Y. Pomeau, J.C. Roux, A. Rossi, S. Bachelart, and C. Vidal, J. Phys. (Paris) **42**, L271 (1981).
- [38] P.S. Linsay, Phys. Rev. Lett. **47**, 1349 (1981).
- [39] J. Testa, J. Perez, and C. Jeffries, Phys. Rev. Lett. **48**, 714 (1982).
- [40] C. Jeffries and J. Perez, Phys. Rev. A **26**, 2117 (1982).
- [41] M. Dubois, M.A. Rubio, and P. Berge, Phys. Rev. Lett. **51**, 1446 (1983).
- [42] W.J. Yeh and Y.H. Kao, Appl. Phys. Lett. **42**, 299 (1983).
- [43] J.Y. Huang and J.J. Kim, Phys. Rev. A **36**, 1495 (1987).
- [44] P. Richetti, P. DeKepper, J.C. Roux, and H.L. Swinney, J. Stat. Phys. **48**, 977 (1987).
- [45] N. Kreisberg, W.D. McCormick, and H.L. Swinney, Physica D **50**, 463 (1991).
- [46] H.G. Schuster, *Deterministic Chaos: an introduction* (Physik-Verlag, Weinheim, Federal Republic of Germany, 1984).
- [47] P. Holmes and F. Diacu, *Intalniri ceresti - originea haosului si a stabilitatii* (Societatea Stiinta si Tehnica SA, Bucuresti, Romania, 1996) p. 150.
- [48] O. Penrose, Rep. Prog. Phys. **42**, 129 (1979).
- [49] A. Atalmi, M. Baldo, G. F. Burgio, and A. Rapisarda, Phys. Rev. C **58**, 2238 (1998).
- [50] A.M. Kowalski, M.T. Martin, J. Nuñez, A. Plastino, and A.N. Proto, Phys. Rev. A **58**, 2596 (1998).
- [51] A. Bialas, in *Proceedings of the NATO-ASI International Summer School "Particle Production Spanning MeV and TeV Energies", Nijmegen, 1999*, edited by W. Kittel, P.J. Mulders, and O. Scholten, NATO Science Series C: Mathematical and Physical Sciences - Vol. 554 (Kluwer Academic Publishers, Nijmegen, The Netherlands, 1999).
- [52] V. Latora and M. Baranger, Phys. Rev. Lett. **82** 520 (1999).
- [53] V. Latora, M. Baranger, A. Rapisarda, and C. Tsallis, Phys. Lett. A **273**, 97 (2000).
- [54] A. Wolf, J.B. Swift, H.L. Swinney, and J.A. Vastano, Physica D **16**, 285 (1985).
- [55] K. Ramasubramanian and M.S. Sriram, Physica D **139**, 72 (2000).